Flavones modulate respiratory epithelial innate immunity: Anti-inflammatory effects and activation of the T2R14 receptor

Benjamin M. Hariri[‡], Derek B. McMahon[‡], Bei Chen[‡], Jenna R. Freund[‡], Corrine J. Mansfield[§], Laurel J. Doghramji,
Nithin D. Adappa[‡], James N. Palmer[‡], David W. Kennedy[‡], Danielle R. Reed[§], Peihua Jiang[§], and ![ORCID] Robert J. Lee[‡¶1]

From the ‡Department of Otorhinolaryngology–Head and Neck Surgery, and the ¶Department of Physiology, University of
Pennsylvania Perelman School of Medicine, Philadelphia and the §Monell Chemical Senses Center,
Philadelphia, Pennsylvania 19104

Edited by Luke O'Neill

Chronic rhinosinusitis has a significant impact on patient quality of life, creates billions of dollars of annual healthcare costs, and accounts for ~20% of adult antibiotic prescriptions in the United States. Because of the rise of resistant microorganisms, there is a critical need to better understand how to stimulate and/or enhance innate immune responses as a therapeutic modality to treat respiratory infections. We recently identified bitter taste receptors (taste family type 2 receptors, or T2Rs) as important regulators of sinonasal immune responses and potentially important therapeutic targets. Here, we examined the immunomodulatory potential of flavones, a class of flavonoids previously demonstrated to have antibacterial and anti-inflammatory effects. Some flavones are also T2R agonists. We found that several flavones inhibit Muc5AC and inducible NOS up-regulation as well as cytokine release in primary and cultured airway cells in response to several inflammatory stimuli. This occurs at least partly through inhibition of protein kinase C and receptor tyrosine kinase activity. We also demonstrate that sinonasal ciliated epithelial cells express T2R14, which closely co-localizes (<7 nm) with the T2R38 isoform. Heterologously expressed T2R14 responds to multiple flavones. These flavones also activate T2R14-driven calcium signals in primary cells that activate nitric oxide production to increase ciliary beating and mucociliary clearance. *TAS2R38* polymorphisms encode functional (PAV: proline, alanine, and valine at positions 49, 262, and 296, respectively) or nonfunctional (AVI: alanine, valine, isoleucine at positions 49, 262, and 296, respectively) T2R38. Our data demonstrate that T2R14 in sinonasal cilia is a potential therapeutic target for upper respiratory infections and that flavones may have clinical potential as topical therapeutics, particularly in T2R38 AVI/AVI individuals.

Chronic rhinosinusitis (CRS)[2] is a syndrome of chronic inflammation and/or infection of the upper respiratory tract, which leads to substantial decreases in patient quality of life, creates >$8 billion in direct healthcare costs in the United States alone, and can seed lower respiratory infections and exacerbate lung diseases (1–3). CRS is also an important public health concern, as it accounts for ~20% of antibiotic prescriptions in adults in the United States (1, 4–8), making it a significant driver for the emergence of antibiotic-resistant organisms (9–15). An attractive therapeutic strategy to avoid the selective pressures for antibiotic resistance is to stimulate endogenous innate host defenses. However, this requires a better understanding of the receptors involved in activating upper airway innate immunity.

It is believed that multiple etiologies contribute to the pathogenesis of CRS, but a common phenotype of the disease is defective mucociliary clearance, the major physical defense of the conducting airways (1, 3). A thin layer of mucus secreted by airway goblet cells and submucosal glands traps inhaled pathogens and particulates. Coordinated beating of motile cilia drives transport of this mucus to the oropharynx, where it is cleared by expectoration or swallowing (16). In CRS, chronic infection and persistent inflammation is associated with stasis of sinonasal secretions, possibly through alterations of basal (17, 18) or stimulated (19) ciliary beat frequency (CBF), mucus viscosity (17, 20), or ion/fluid transport (21). Enhancing mucociliary clearance may have potential therapeutic benefit for CRS patients (1, 3).

ASBMB

We previously showed that a bitter "taste" G-protein-coupled receptor, T2R38, is expressed in the motile cilia of cells of the upper airway (nose and sinuses) and modulates mucociliary clearance through calcium (Ca^{2+})-dependent production of nitric oxide (NO) (2, 22–27). Our data suggest that T2R38 is activated by acyl-homoserine lactone (AHL) quorum-sensing molecules secreted by Gram-negative bacteria (27), including the common airway pathogen *Pseudomonas aeruginosa*. When activated, T2R38-activated NO production drives an increase in CBF through protein kinase G (PKG), which phosphorylates ciliary proteins (28). This NO also directly diffuses into the airway surface liquid with antibacterial effects (27). Because NO damages the cell walls and DNA of bacteria (29, 30), NO production by the sinonasal epithelium is thought to be important for preventing infection. Supporting this, nitric-oxide synthase (NOS) polymorphisms have been associated with severe CRS (31). We found that patients homozygous for a polymorphism in the *TAS2R38* gene resulting in non-functional T2R38 protein (the AVI (alanine, valine, isoleucine at positions 49, 262, and 296, respectively) polymorphism (32)) are more susceptible to Gram-negative bacterial infection (27), have a higher incidence of biofilm-forming bacteria (33), are at higher risk for CRS requiring functional endoscopic sinus surgery (FESS) (34, 35), and may have worse outcomes after FESS for CRS without nasal polyps (36) compared with patients homozygous for the functional (PAV: proline, alanine, and valine at positions 49, 262, and 296, respectively) allele of *TAS2R38*. There are 25 different T2R bitter receptors in humans (22, 24, 37, 38), and other researchers have confirmed that polymorphisms in at least two *TAS2R* genes, *TAS2R38* and *TAS2R13*, correlate with CRS by genome-wide association (39).

The full picture of T2R38's role in sinonasal immunity in different patient populations is still being elucidated. A subsequent study found no correlation of *TAS2R38* genotype with CRS in Italian patients (40), but this population had different clinical characteristics (*e.g.* more recalcitrant disease and stronger Th2 inflammatory phenotype) than our own studies. A more recent study supported a correlation between *TAS2R38* genotype and CRS severity in a Polish population (41), and an Australian study concluded that AVI/AVI *TAS2R38* is predictive of the presence of culturable bacteria in CRS patient sinuses (42). Moreover, a recent study reported that T2R10 and T2R14, but not T2R38, respond to some AHLs when expressed in HEK293 cells (43). The reason for this discrepancy is not yet clear, although other studies have suggested that T2R38 is indeed important for immune cell detection of AHLs (44, 45). Understanding the full range of T2Rs endogenously expressed by primary differentiated cell types as well as their oligomerization properties will help clarify the best therapeutic compounds to target these receptors to stimulate innate immune responses.

Plants produce thousands of polyphenolic flavonoids (46–49), which are of great biomedical interest, because they have effects on both eukaryotic and prokaryotic cells (47–58). Flavones are a sub-group of flavonoids that have been demonstrated to have antibacterial, antioxidant, and anti-inflammatory effects in various *in vitro* models (48, 51, 53, 55, 57, 59, 60). Moreover, the flavones chrysin and apigenin activate T2R14 and T2R39 (61, 62). Because of their potential antibacterial
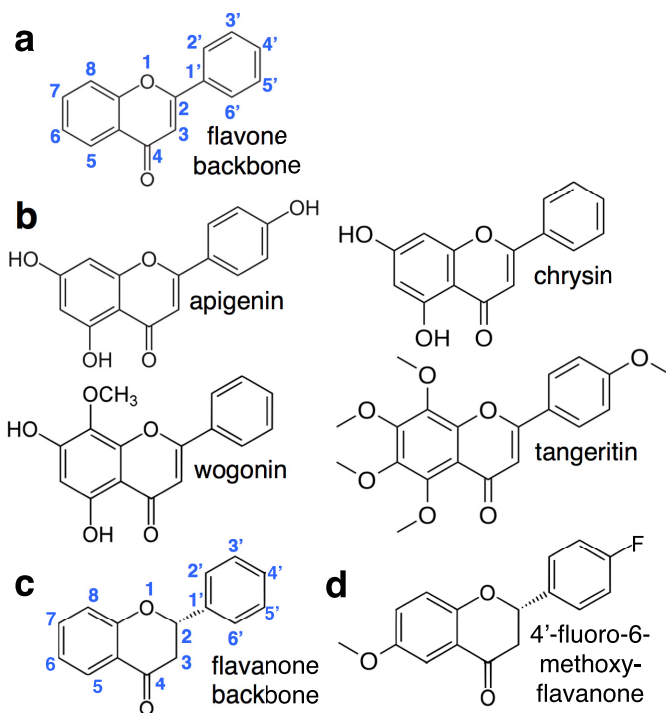
Figure 1. Molecular structures of flavonoids used in this study. *a*, backbone flavone structure. *b*, structures of specific flavones used here: apigenin (4′,5,7-trihydroxyflavone), wogonin (5,7-dihydroxy-8-methoxyflavone), chrysin (5,7-dihydroxyflavone), and tangeritin (4′,5,6,7,8-pentamethoxyflavone). *c*, backbone flavanone structure. *d*, structure of 4′-fluoro-6-methoxyflavanone.

properties, and because multiple *TAS2R* polymorphisms have been linked to CRS (39), we sought to investigate the effects of flavones on airway epithelial cells. We previously examined a separate flavonoid class, anthocyanidins, and found that they did not activate sinonasal cilia T2Rs (58). However, anthocyanidins have a $\geq$1-log higher effective concentration (EC) for T2R activation than flavones (*e.g.* 250 μM EC for the anthocyanidin cyanidin *versus* 8 μM EC for the flavone apigenin for T2R14) (61, 62). The goal of this study was to begin to investigate the potential role of flavones as a treatment for upper respiratory infections, with a special focus on their anti-inflammatory properties as well as potential reactivity with upper airway T2Rs.

Results

Flavones have anti-inflammatory effects in airway epithelial cells

Several representative flavones (backbone structure shown in Fig. 1*a*) were tested, including apigenin (Fig. 1*b*) from bee propolis (50) and wogonin (Fig. 1*b*) from *Scutellaria baicalensis*, one of the 50 fundamental herbs of traditional Chinese medicine (63). Chrysin (Fig. 1*b*), from *Passiflora* flowers (48, 51), and tangeritin (Fig. 1*b*), found in citrus peels (48, 51), were also used. We also used a structurally related flavanone, the backbone of which is a stereoisomer of the flavone backbone (Fig. 1*c*). Substituted methoxyflavanones, including 4′-fluoro-6-methoxyflavanone, have been suggested to inhibit both T2R39 and T2R14 (64, 65).
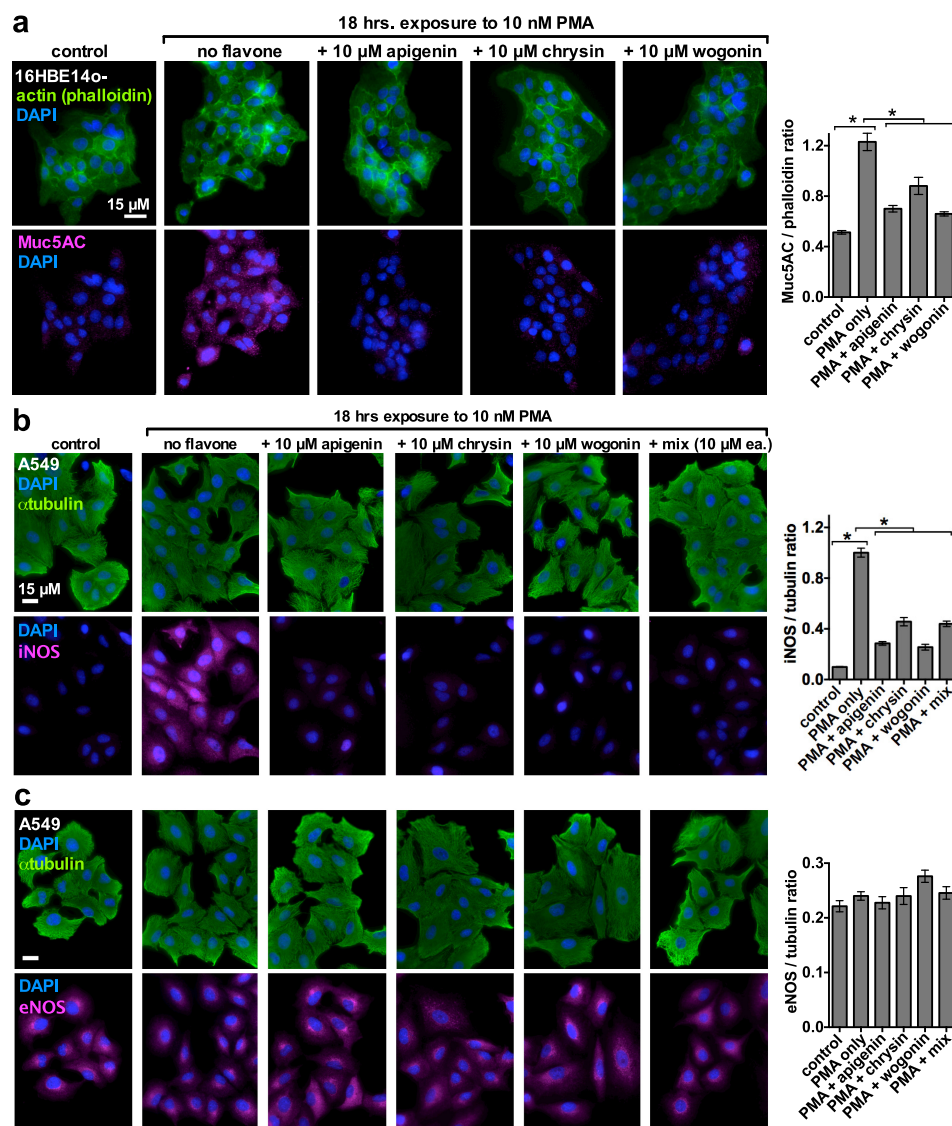
**Figure 2. Apigenin, chrysin, and wogonin reduce Muc5AC up-regulation in 16HBE bronchial epithelial cells and iNOS-up-regulation in A549 lung epithelial cells stimulated with a protein kinase C agonist.** *a, left images* show actin (AlexaFluor 488-labeled phalloidin; *green*) and Muc5AC immunofluorescence (*magenta*) in untreated (*control*) 16HBE cells as well as cells treated with 10 nm PMA for 18 h in the absence or presence of flavones as indicated. Muc5AC immunofluorescence was normalized to phalloidin fluorescence (40–100 cells quantified from at least two separate experiments for each condition). *b, left* shows α-tubulin (*green*) and iNOS (*magenta*) immunofluorescence in A549 cells under similar conditions to *a. Right* shows quantification of iNOS/α-tubulin fluorescence ratio (30–110 cells quantified from at least two separate experiments for each condition). *c, left* shows α-tubulin (*green*) and eNOS under conditions as in *b. Right graph* shows eNOS/α-tubulin fluorescence ratio. *Asterisks* denote significance between *bracketed groups* (one-way ANOVA, Bonferroni post-test; *, $p < 0.05$); data values from *bar graphs* are reported in supplemental Material.

We sought to determine whether flavones exhibited anti-inflammatory effects in airway epithelial cells, as reported previously in other cell types (51). The protein kinase C (PKC) pathway is utilized by many inflammatory mediators, and activation of PKC with phorbol 12-myristate 13-acetate (PMA) is frequently used to induce inflammatory effects *in vitro*. PKC inhibitors are utilized as anti-inflammatory compounds in a number of diseases of chronic inflammation (66–68). Apigenin and other flavones may have PKC inhibitory activity (69, 70), suggesting they may be useful for attenuating PKC-dependent inflammatory effects. When 16HBE14o− (16HBE) airway epithelial cells were stimulated with PMA (10 nm, 18 h), we observed a marked up-regulation of Muc5AC expression via immunofluorescence microscopy (Fig. 2*a*). Muc5AC is a gel-forming mucin in the airway, and Muc5AC up-regulation is a

common hallmark of chronic obstructive pulmonary disease and other inflammatory airway diseases (71, 72). Other studies have also demonstrated that PKC up-regulates Muc5AC (73). Individual flavones (10 μM each) significantly repressed PMA-induced Muc5AC up-regulation (Fig. 2*a*), suggesting they may have an anti-inflammatory role in airway cells.

We tested another important marker of inflammation, inducible nitric-oxide synthase (iNOS) (74–77). Whereas acute NO production can be antibacterial, chronic excessive NO production through transcriptional up-regulation of iNOS may exacerbate and prolong inflammation. PMA induced an up-regulation of iNOS in A549 alveolar-derived airway cells (Fig. 2*b*) that was likewise reduced with individual flavone compounds (10 μM each; Fig. 2*b*). As a control for the specificity of iNOS as an inflammatory marker, we examined changes in
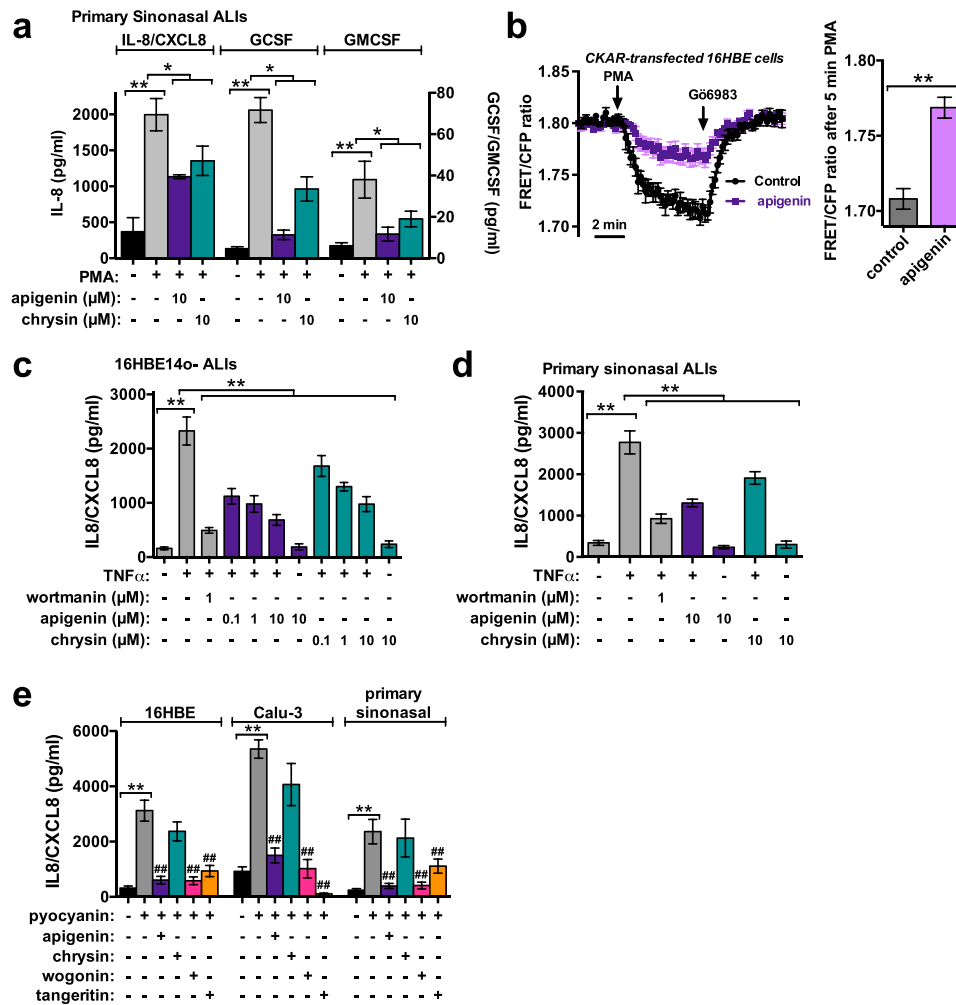
Figure 3. Flavones reduce cytokine release from 16HBE14o−, Calu-3, and primary sinonasal ALI cultures. *a*, release of IL-8, GCSF, and GMCSF from primary sinonasal ALIs assayed by ELISA. *b*, traces of CKAR FRET/CFP emission ratio from transfected 16HBE cells (*n* = 6–8 experiments for each condition) under control conditions or pre-treated with apigenin for 1 h prior to experiment. Cells were stimulated with PKC-activating PMA (10 μM) followed by the global PKC inhibitor Gö6983 (10 μM). *c* and *d*, similar experiments performed with 16HBE ALIs (*c*) and primary sinonasal ALIs (*d*) stimulated with TNFα (10 ng/ml; 24 h) in the presence or absence of apigenin or chrysin. *e*, IL-8 release (pg/ml) in response to pyocyanin in 16HBE, Calu-3, and primary sinonasal ALI cultures (*n* = 5 ALIs for each condition). Significance was determined by one-way ANOVA, Tukey-Kramer, or Bonferonni post-test; *, *p* < 0.05; **, *p* < 0.01 for all graphs, and for *D*, ##, *p* < 0.01 *versus* pyocyanin alone. Data values from *bar graphs* are reported in supplemental Material.

endothelial NOS (eNOS), typically not up-regulated during inflammation. Immunofluorescence for eNOS exhibited a perinuclear Golgi-like localization, as reported previously (78, 79). PMA had no effect on eNOS, either alone or in the presence of flavones (Fig. 2*c*).

We also directly quantified cytokines released from air-liquid interface (ALI) cultures of primary human sinonasal cells. ALIs from primary cells differentiate into ciliated and goblet cells mimicking the *in vivo* epithelium (24, 27, 80, 81). Primary sinonasal ALIs were stimulated as above with PMA on the apical side in the presence or absence of chrysin or apigenin (Fig. 3*a*). Levels of secreted interleukin-8 (IL-8), granulocyte colony-stimulating factor (GCSF), and granulocyte macrophage colony-stimulating factor (GMCSF) were quantified from basolateral media by ELISA. PMA induced robust secretion of all three cytokines (Fig. 3*a*), and exposure to apigenin or chrysin reduced cytokine release (Fig. 3*a*). To test whether flavones have direct inhibitory activity against PKC, we expressed a PKC FRET-reporter construct, CKAR (82, 83), in 16HBE

cells. CKAR includes the FHA2 domain of RAD53p and a PKC phosphorylation sequence sensitive to all PKC isoforms, flanked by an N-terminal enhanced CFP and C-terminal citrine YFP. When phosphorylated, a reversible conformational change moves the CFP and YFP apart, decreasing FRET emission. A decrease in FRET emission thus correlates with increased PKC activity and vice versa. Single transfected cells were imaged, and the ratio of FRET to CFP emission at CFP excitation is reported, as described previously (80). We noted that cells pretreated for 1 h with 50 μM apigenin exhibited a reduced PKC activation (FRET decrease) in response to 1 μM PMA (Fig. 3*b*).

We likewise examined IL-8 secretion in both 16HBE ALIs (Fig. 3*c*) and primary sinonasal ALIs (Fig. 3*d*) in response to tumor necrosis factor α (TNFα) stimulation. The flavonol quercetin was reported to reduce TNFα-induced IL-8 secretion in 16HBE cells through a phosphatidylinositol 3-kinase (PI3K)-dependent pathway (84). We found that TNFα induced IL-8 secretion ~10-fold in both 16HBE (Fig. 3*c*) and primary sino-
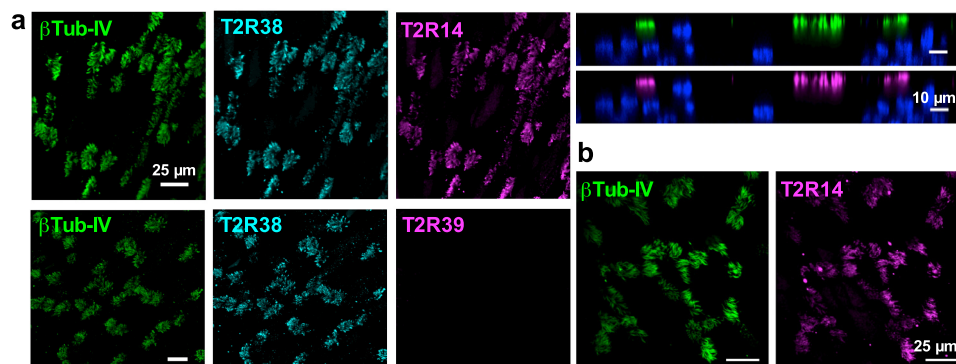
Figure 4. Immunofluorescence co-localization of endogenous T2R38 and T2R14 in sinonasal cilia. *a, upper panels* show a representative confocal immunofluorescence image of a primary sinonasal ALI culture and co-localization of the motile cilia marker β-tubulin IV (*β-TubIV, green*) with T2R38 (*cyan*) and T2R14 (*magenta*). Detection of T2R39 was not observed (*lower panels*). Orthogonal slice of T2R14 and β-tubulin IV is shown at *top right*. *b*, T2R14 immunofluorescence was observed in non-permeabilized cells using an antibody recognizing an extracellular epitope, supporting surface localization; β-tubulin IV staining was conducted after subsequent second fixation and permeabilization. Images are representative of results observed with ALI cultures from at least three individual patients.

nasal ALIs (Fig. 3*d*), which was inhibited by the PI3K inhibitor wortmannin (Fig. 3, *c* and *d*). Apigenin and chrysin had no effects on IL-8 secretion alone, but both compounds dose-dependently reduced IL-8 secretion in response to TNFα (Fig. 3, *c* and *d*).

We also tested the effects of flavones on IL-8 secretion induced by *Pseudomonas* pyocyanin (85). The isoflavone genistein was previously shown to inhibit pyocyanin-induced IL-8 secretion (85), likely via genistein's ability to inhibit tyrosine kinase activity (69, 86–88). We observed induction of IL-8 after treating 16HBE or Calu-3 ALIs with 25 μM pyocyanin for 24 h. Apigenin (89–91), wogonin (91–94), and tangeritin (95–97) have previously also been shown to inhibit tyrosine kinases, whereas chrysin has a less inhibitory effect (88, 98). Fitting with these prior observations, pyocyanin-induced IL-8 secretion was reduced in the presence of apigenin, wogonin, and tangeritin but not chrysin (Fig. 3*e*).

### Flavones activate T2R14 expressed in sinonasal epithelial cell cilia

The above data suggest that flavones modify sinonasal epithelial inflammation-induced up-regulation of Muc5AC, iNOS, and cytokines. As mentioned above, apigenin and chrysin may also activate T2R14 and T2R39 (61), whereas tangeritin may activate T2R14 and T2R46 but not T2R39 (99). We hypothesized that flavones may activate one or more of these T2Rs located in the upper respiratory epithelium (22, 25). The molecular structures of flavones were examined using BitterX, an open-access platform for predicting whether a molecule is bitter as well as predicting which T2R receptors are likely to respond (100). BitterX identified T2R14 and T2R39 as having the highest probabilities of being activated by all flavone molecules examined here (supplemental Table 1).

We examined endogenous T2R14 and T2R39 expression in primary sinonasal ALIs with anti-C-terminal antibodies validated against cross-reactivity by heterologous expression of T2R14 and T2R39 in A549 cells (supplemental Fig. 1). Using these antibodies, we detected endogenous expression of T2R14 but not T2R39 in primary sinonasal ALIs (Fig. 4*a*). T2R14 co-localized with the motile cilia marker βTubulin IV and T2R38

(Fig. 4*a*), previously demonstrated to be localized to sinonasal cilia (27). Surface localization of T2R14 was confirmed by staining un-permeabilized cells with an antibody raised against an epitope (amino acids 213–262) containing an extracellular loop between transmembrane helix 6 and 7 (Fig. 4*b*). The co-localization observed between T2R38 and T2R14 was highly distinct from the pattern observed with T2R38 or T2R14 and T2R4. T2R4 localized only to the distal tips of cilia (supplemental Fig. 2, *a* and *b*). This distal localization of T2R4 was previously observed in bronchial cilia (101), and it may be related to previous HEK293T heterologous expression data suggesting that recombinant T2R4 does not oligomerize with T2R14 or T2R38, whereas T2R14 and T2R38 can oligomerize with each other (102, 103). T2R14 and T2R38 co-localization was similar to that observed with T2R16 (supplemental Fig. 2, *c* and *d*).

We tested the ability of the flavone compounds to activate recombinant T2Rs4, -5, -14, -38, -39, and -16 by expressing these T2Rs in HEK293T cells with a Ca²⁺-activating Gα chimera, Gα$_{16}$-gust44, a Gα$_q$ fused to the last 44 amino acids of gustducin that couples to T2Rs, a commonly used method to test T2R activation (104). HEK293T cells expressing T2R14 + Gα16-gust44, but not Gα16-gust44 alone, exhibited robust intracellular Ca²⁺ ([Ca²⁺]$_i$) responses to all flavones tested (supplemental Fig. 3). We found no responses to apigenin in cells transfected with T2R4, -5, 16, or -38, despite robust responses to known cognate ligands (supplemental Fig. 4). T2R39 did respond to apigenin (supplemental Fig. 4), as predicted.

Because endogenous T2R14 and T2R38 appeared to strongly co-localize, and because the primary antibodies used here were both raised against the C termini (Fig. 5*a*), we examined whether endogenously expressed T2R38 and T2R14 interacted closely enough to observe Förster (also known as fluorescence) resonance energy transfer (FRET; schematic shown in Fig. 5*b*) in primary sinonasal ALIs. FRET is a highly quantitative measure of co-localization. Although T2Rs have been previously proposed to oligomerize, presumably as dimers (102, 103), these studies have been done in heterologous overexpression HEK293 cell systems, and thus results must be interpreted with
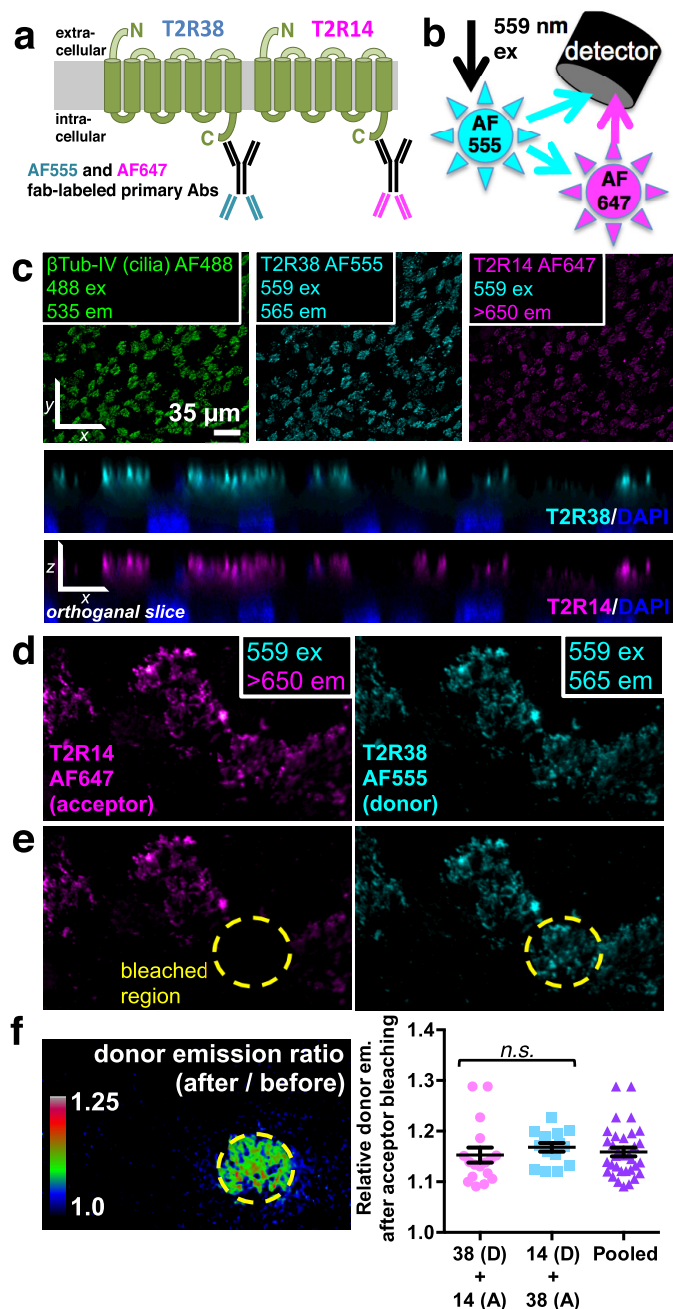
Figure 5. Demonstration of a close co-localization of endogenously expressed T2R38 and T2R14 in sinonasal cilia by FRET. *a*, antibody labeling FRET strategy. *b*, diagram of basic principle of FRET. *c*, *x-y* plane images (*top*) and *x-z* plane image (orthogonal view; *bottom*) of T2R14-AF647 FRET upon T2R38-AF555 excitation. *d* and *e*, images showing T2R14 and T2R38 immunofluorescence signals before (*d*) and after (*e*) acceptor photobleaching (via 647 laser and tornado bleaching function in Olympus Fluoview; photo-bleached area shown in *yellow circle*). *f*, *left panel* shows ratio image showing increase in donor fluorescence after acceptor bleaching. *Right panel* shows relative change in donor emission under two conditions (T2R14 acceptor + T2R38 donor, as shown, and T2R38 acceptor + T2R14 donor) as well as pooled data. *n.s.,* not significantly different.

caution. Overexpression can force molecules to interact *in vitro* that may not necessarily interact *in vivo* at endogenous expression levels. These results must be interpreted in light of findings from studies of endogenous expression.

We used AlexaFluor (AF) 555 and AF647 as our FRET pair (Förster radius [R_o] = 51 Å). Primary antibodies were labeled

with AF-conjugated Fab fragments. We noted a significant T2R14 FRET signal in the AF647 emission channel when T2R38 AF555 was excited using a 559-nm laser (Fig. 5*c*). Similar T2R38 FRET signals were observed when T2R14 was labeled with AF555 and T2R38 was labeled with AF647. When the acceptor fluorophore was bleached using a 647 laser, donor fluorescence increased (Fig. 5, *d–f*). Quantification of the relative increase in donor fluorescence after acceptor bleaching allows calculation of the FRET efficiency (E). E was measured to be 15 ± 3% when T2R38 was the donor and T2R14 was the acceptor, 17 ± 1% when T2R14 was the donor and T2R38 was the acceptor, and 16 ± 2% when the two conditions were pooled. R_o is the distance at which the E is 50% (51 Å for AF555 and AF647); FRET efficiency decreases to the 6th power as distance (R) increases: $R = R_o \cdot ((1 - E)/E)^{1/6}$. Thus, with 0.16 E, $R = 51 \text{ Å} \cdot ((1 - 0.16)/0.16)^{1/6} = 67$ Å. Although we cannot conclude that the two proteins form oligomers *per se* from our data due to the sizes of the antibodies involved in our measurements, similar antibody-based FRET measurements have been used to suggest a "close association" of endogenously expressed proteins (105). These quantitative FRET measurements demonstrate a close co-localization of T2Rs to a higher resolution (~7 nm) than yet achievable by most current super-resolution light microscopy techniques (106).

With the knowledge that T2R14 is endogenously expressed in primary sinonasal ciliated epithelial cells and the knowledge that this receptor is activated by flavones, we sought to determine whether flavones activate T2R14-dependent Ca^{2+}-driven nitric oxide (NO) responses in these cells, as demonstrated previously with T2R38 (27). Apigenin and chrysin activated low-level Ca^{2+} responses (Fig. 6, *a–c*) identical to what was previously observed with stimulation of sinonasal cilia-localized T2R38 (27). Although these $[Ca^{2+}]_i$ changes are small, it is important to note that these are measurements of global $[Ca^{2+}]_i$; localized responses at or near the apical membrane and/or within cilia could be much higher (107). Importantly, the ECs observed here fit with ECs previously determined for these compounds for heterologously expressed T2R14 (8 μM for apigenin and 63 μM for chrysin (61, 62)). These responses were also blocked in the presence of 4′-fluoro-6-methoxyflavanone (Fig. 6, *d* and *e*), a previously identified T2R14 inhibitor (64, 65). We found that 4′-fluoro-6-methoxyflavanone inhibited apigenin-induced T2R14 $[Ca^{2+}]_i$ responses at 50 μM but had activating effects at higher concentrations, suggesting that 4′-fluoro-6-methoxyflavanone may act as a partial agonist rather than a competitive antagonist (supplemental Fig. 5). Nonetheless, this inhibition in primary cells supports that these responses are mediated by T2R14. No difference in $[Ca^{2+}]_i$ responses was observed when cultures from T2R38 PAV/PAV (homozygous taster) or AVI/AVI (homozygous non-taster) individuals were compared, suggesting that, despite close co-localization and possible heterodimerization, the non-functional AVI T2R38 does not adversely affect T2R14 Ca^{2+} signaling in cilia (supplemental Fig. 6, *a, b, and e*). Supporting this, we found no inhibition of apigenin-induced Ca^{2+} responses with the T2R38 inhibitor probenecid (1 mM) (108) and no inhibition of phenylthiocarbamide-induced Ca^{2+} responses in PAV/PAV cultures with 4′-fluoro-6-methoxyflavanone (supplemental Fig. 6, *c–e*).
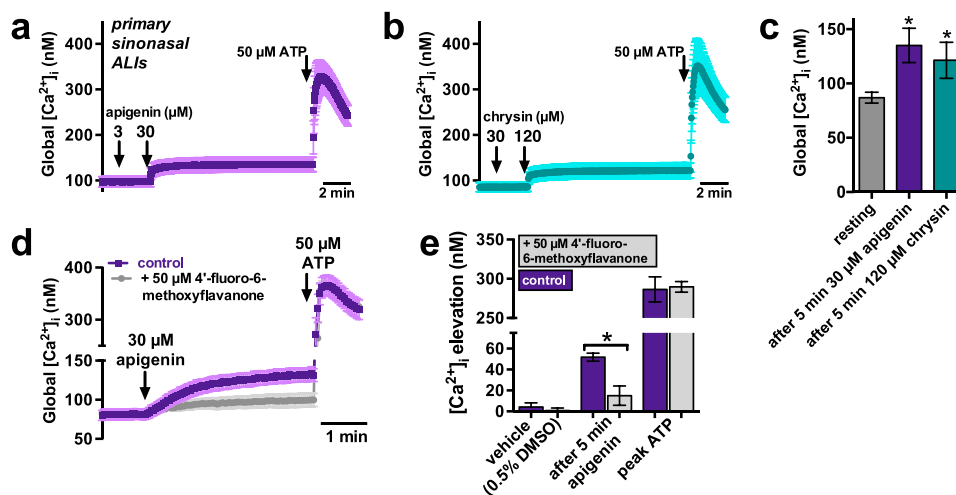
Figure 6. Flavone-activated Ca²⁺ signaling in primary sinonasal ALIs. *a* and *b*, low-level Ca^{2+} responses in primary sinonasal ALIs in response to apigenin (*a*) and chrysin (*b*). *c*, *bar graph* summarizing $[Ca^{2+}]_i$ from *a* and *b*. *d*, $[Ca^{2+}]_i$ elevations were blocked in the presence of T2R14 antagonist 4′-fluoro-6-methoxyflavanone (5 min pre-treatment, followed by stimulation in the continued presence of 4′-fluoro-6-methoxyflavanone). *e*, *bar graph* shows change in $[Ca^{2+}]_i$ from *d*. Significance determined by one-way ANOVA with Tukey-Kramer (*c*) or Bonferroni (*d*) post-test; *, $p < 0.05$ and **, $p < 0.01$. Data values from *bar graphs* are reported in supplemental Material.

Activation of T2R14 in sinonasal cilia results in NO production and increases ciliary beat frequency

As observed with T2R38, flavone/T2R14-induced Ca^{2+} responses were associated with increases in fluorescence of DAF-FM, which reacts with intracellular reactive nitrogen species (Fig. 7*a*). DAF-FM fluorescence increases reflected NO production, as they were blocked by the nitric-oxide synthase (NOS) inhibitor L-N^G-nitroarginine methyl ester (L-NAME) but not by its inactive analogue D-NAME (Fig. 7*b*). These responses were blocked by the phospholipase C inhibitor U73122 but not by its inactive analogue U73343 (Fig. 7*c*). Like flavone-induced Ca^{2+} signals, flavone induced NO production was also inhibited by 4′-fluoro-6-methoxyflavanone (Fig. 7*d*). These results are summarized in Fig. 7*e*.

Abolishment of Ca^{2+} signaling by pre-loading cells with a Ca^{2+} chelator (10 μM BAPTA-AM for 30 min) followed by stimulation with apigenin or chrysin under extracellular Ca^{2+}-free conditions (Ca^{2+}-free solution containing 2 mM EGTA) likewise abolished NO production (Fig. 7*g*). We also tested a structurally unrelated T2R14 agonist, niflumic acid (NFA; 50 μM; EC ~5 μM for T2R14) (109), which also activated NO production (Fig. 7*g*).

The constant and coordinated beating of airway motile cilia drives mucociliary clearance (1, 3, 110, 111). Because NO is known to increase ciliary beating through activation of guanylyl cyclase and production of cGMP (27, 28), we measured CBF during stimulation with apigenin or chrysin. Both compounds increased CBF (Fig. 8*a*; $n = 6-8$ ALIs from at least three patients per condition). The increases in CBF were dependent on NO production, as they were blocked by L-NAME but not by D-NAME (Fig. 8*b*).

Discussion

This study first demonstrates that flavones have anti-inflammatory effects on Muc5AC and iNOS up-regulation as well cytokine secretion in airway epithelial cells. This supports prior studies that apigenin, chrysin, and wogonin inhibit Muc5AC

up-regulation in NCI-H292 bronchial cancer cells in response to epidermal growth factor (91, 112, 113) or TNFα (114, 115). Our data suggest this occurs partly through direct inhibition of kinase C rather than upstream or downstream mechanisms, as they were directly able to block PKC activity in response to PMA. We also demonstrate relevance of prior findings from cell lines to primary well differentiated airway epithelial cells. We postulate that flavones may be useful potential anti-inflammatory mediators in airway diseases, as has also been suggested for the related, but structurally different, flavonol quercetin (84).

Second, we demonstrate that flavones activate T2R14 in primary sinonasal epithelial cell cilia. T2R14 is also expressed in bronchial cilia (101) and airway smooth muscle cells (116). This is the first demonstration of T2R14 in sinonasal cilia, and the finding that T2R14 closely co-localizes (<7 nm) with T2R38 is important and novel. These studies were facilitated by the commercial availability of valid and specific antibodies directed at moieties on the same side of the plasma membrane. Although we cannot directly determine whether these T2Rs oligomerize by the methods used here due to the size of the labeled antibodies, this study is one of the first to demonstrate such a close interaction with endogenously expressed T2Rs. Previous studies of T2R interactions have been carried out in heterologous expression HEK293 models (102, 103). Results from such models, where overexpression may induce interactions that do not normally occur at physiological protein levels, must be interpreted with caution and must be verified in more differentiated *in vitro* models and/or tissues. Future studies in airway epithelial cells may help to clarify the oligomerization properties of the subset of T2Rs endogenously expressed in motile cilia, shedding important light into the cell biology of these receptors. Although T2R38 is required for AHL detection in sinonasal epithelial cells (27) and immune cells (44, 45), another study has suggested T2R10 responds to AHLs in a heterologous expression system (43). Oligomerization has substantial functional consequences for many G-protein-coupled receptors
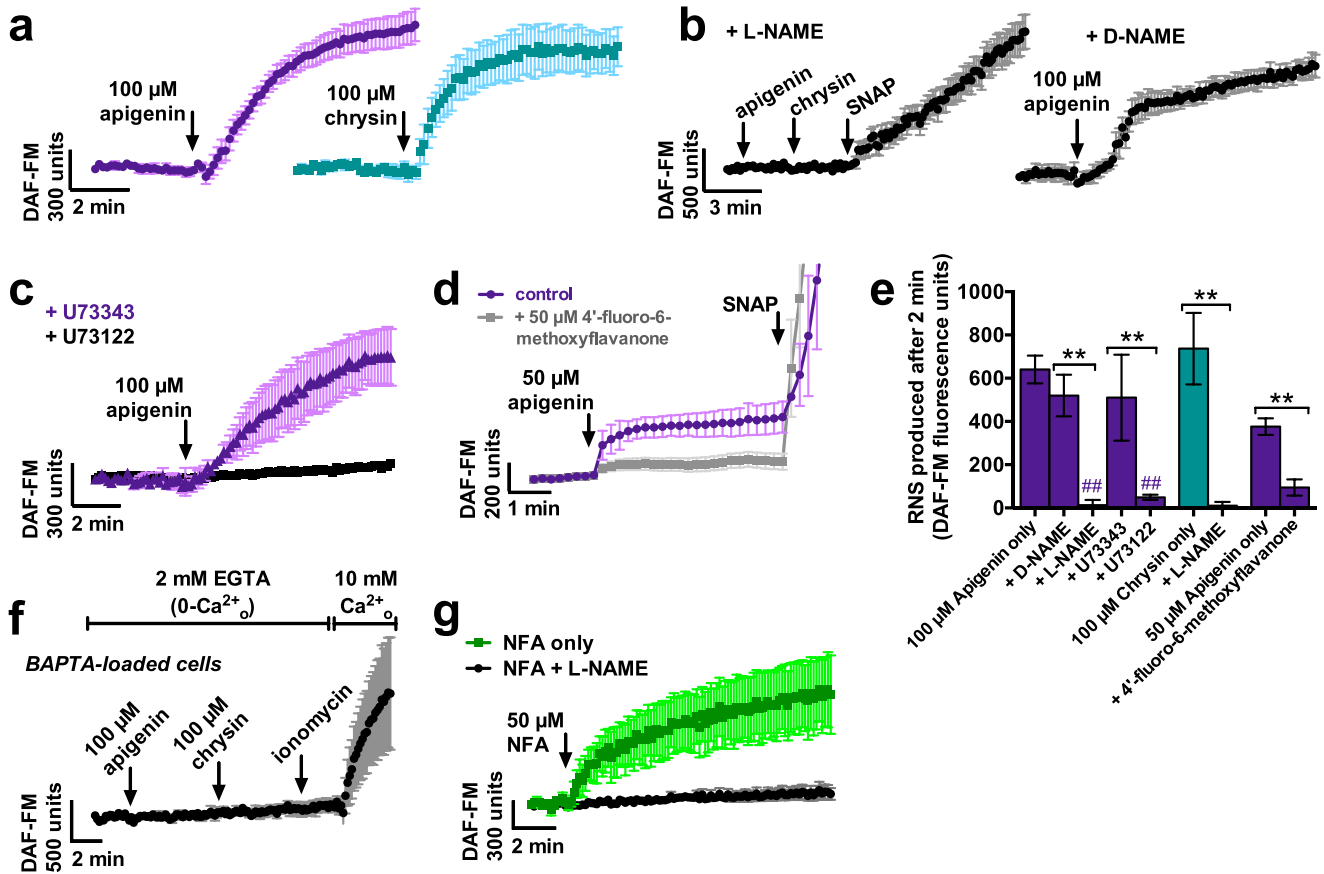
Figure 7. Flavones regulate sinonasal epithelial Ca²⁺-dependent NO production. *a*, DAF-FM fluorescence increases, reflecting production of reactive nitrogen species, in response to apigenin and chrysin. *b*, inhibition of DAF-FM fluorescence increases by NOS inhibitor L-NAME but not by inactive analogue D-NAME. *c*, inhibition of DAF-FM fluorescence increases by phospholipase C inhibitor U73122 but not by inactive analogue U73343 (10 μM applied apically; 60 min pre-treatment). *d*, trace of NO production in the absence (*control*) or presence of 4′-fluoro-6-methoxyflavanone. *e*, *bar graph* showing DAF-FM data from *b* to *d*. Significance was determined by one-way ANOVA, Tukey-Kramer post-test. *Asterisks* denote significance between *bracketed groups* (**, $p < 0.01$) and ##, $p < 0.01$ *versus* apigenin or chrysin only (*control*). *f*, inhibition of DAF-FM fluorescence increases after inhibition of Ca²⁺ signaling by loading of cells with BAPTA in the presence of Ca²⁺-free extracellular solution containing 2 mM EGTA. *g*, DAF-FM fluorescence traces in response to the T2R14 agonist NFA in the absence or presence of L-NAME. All traces are the means ± S.E. of at least four experiments using cultures from at least three individual patients. Data values from *bar graphs* are reported in supplemental Material.
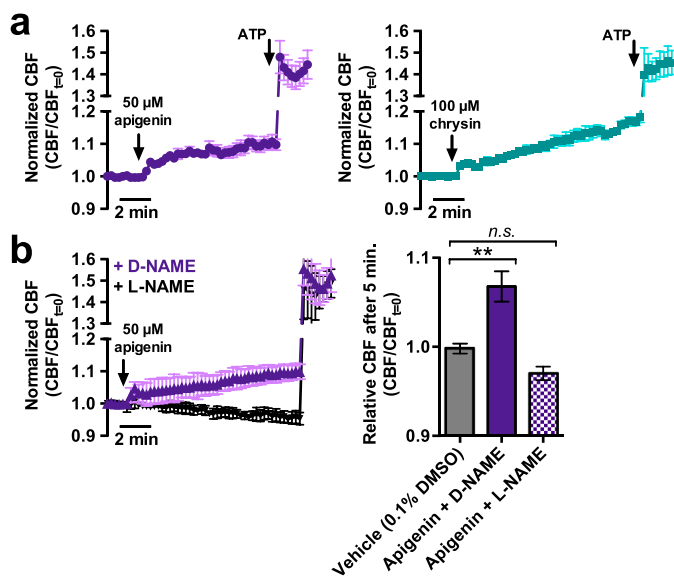
Figure 8. Flavones increase sinonasal ciliary beat frequency in an NO-dependent manner. *a*, CBF increase in response to apigenin and chrysin. *b*, inhibition of apigenin-activated CBF increase by L-NAME but not D-NAME. Significance determined by one-way ANOVA with Tukey-Kramer post-test (**, $p < 0.01$).

(117, 118). A better understanding of the oligomerization of endogenous T2Rs, both with other T2Rs as well as with other receptor classes (116), may help explain some such discrepancies that exist in the literature.

Activation of T2R14 results in similar Ca²⁺-dependent NO production and ciliary beat increases to those observed during T2R38 stimulation (27). These CBF increases were smaller than those observed with ATP but were sustained and were similar to elevations previously observed with T2R38 stimulation (27) that may have clinical relevance (27, 34–36, 39, 41, 42, 119).

Quercetin was previously shown to increase CBF in primary human sinonasal cells (120), and our data suggest this activation may at least partly occur through activation of T2R14. Interestingly, T2R14 is activated by several other compounds that have been used clinically, including NFA, the antihistamine diphenhydramine, the non-steroidal anti-inflammatory drug flufenamic acid, and quercetin (62). NFA is commonly used experimentally at high micromolar-to-low millimolar concentrations as a Ca²⁺-activated Cl⁻ channel blocker (121–126). NFA was shown to activate Ca²⁺ release from intracellular stores in rat pulmonary artery smooth muscle cells (127); as bronchial smooth muscles express T2R14 (116, 128), arterial

smooth muscle expression of T2R14 may explain this effect. Off-target T2R effects of NFA should be taken into account when using this compound with cells that express T2R14. It is also likely that there is either an endogenous host ligand or a pathogen ligand for physiological activation of sinonasal T2R14, which remains to be identified. Screening of bacterial or fungal compounds against this protein may reveal the identity of such a compound and help clarify the physiological role of T2R14 in sinonasal innate immunity.

We previously postulated that T2R38 may be a useful therapeutic target to activate NO-driven endogenous innate immune responses in patients to treat airway infections without the use of antibiotics (2, 22, 25–27, 129). However, there is a high frequency of non-functional (non-taster) *TAS2R38* polymorphisms. In Caucasians, ~25% of the population is homozygous for the AVI non-functional *TA2R38* (27, 32, 130–132). These patients would be expected to be completely non-responsive to T2R38-directed therapeutics, and we have previously confirmed that ALIs grown from AVI/AVI patients do not respond to T2R38 agonists (27). The observation that T2R14 activates a highly similar set of responses from both T2R38 PAV/PAV and AVI/AVI sinonasal cells suggests that T2R14 may be a viable therapeutic target to activate innate immune pathways in T2R38 AVI/AVI patients. However, polymorphisms in *TAS2R14* also exist (133), although their effects are not as well studied. Future work is needed to understand how known *TAS2R14* polymorphisms affect T2R14 function. Additionally, identifying the full gamut of sinonasal cilia taste receptors will allow elucidation of agonist mixtures that activate multiple sinonasal T2Rs to achieve maximum possible benefit in the largest patient population possible. T2R agonists such as flavones that have additional beneficial non-T2R-dependent effects (*e.g.* PKC inhibition) may increase efficacy of this therapeutic strategy.

Experimental procedures

Reagents and solutions

Unless indicated, all reagents and solutions used were as described previously (23, 24, 27, 80, 81). Fura-2-AM, DAF-FM-DA, and BAPTA-AM were from Invitrogen. Flavones, phorbol 12-myristate 13-acetate (PMA), L- and D-N^G-nitroarginine methyl ester (L-NAME and D-NAME), ionomycin, U73122, and U73343 were from Cayman (Ann Arbor, MI), and 4′-fluoro-6-methoxyflavanone (2-(4-fluorophenyl)-6-methoxychroman-4-one) was purchased from VitaScreen, LLC (Urbana-Champaign, IL). Anti-T2R38 (ab130503; rabbit polyclonal), anti-β-tubulin IV (ab11315; mouse monoclonal), anti-T2R16 (ab75106 rabbit polyclonal), and anti-Muc5AC (ab3649; mouse monoclonal) primary antibodies were from Abcam (Cambridge, MA). Anti-T2R14 (PA5-39710; rabbit polyclonal) and T2R39 (PA5-39711; rabbit polyclonal) primary antibodies were from Thermo Fisher Scientific (Waltham, MA). Anti-α-tubulin (12G10; mouse monoclonal) antibody was from Developmental Studies Hybridoma Bank (University of Iowa, Iowa City). Anti-iNOS (sc-654; rabbit polyclonal) and T2R4 (T13, sc169494; goat polyclonal) were from Santa Cruz Biotechnology. Anti-eNOS antibody (NB-300-605; rabbit polyclonal) was from Novus (Littleton, CO). Anti-T2R14, amino acids 229–278 (LS-C120957; rabbit polyclonal), was from (LSBio, Seattle WA). ELISAs for GCSF and GMCSF were from PeproTech (Rocky Hill, NJ); ELISA for IL-8 was from Thermo Fisher Scientific. ELISAs were carried out according to the manufacturers' instructions. Unless indicated below, all other reagents were from Sigma. Stock solutions of flavones were made at 100 or 120 mM in DMSO; working solutions contained ≤0.1% DMSO and were made immediately before use. CKAR expression vector was obtained from Alexandra Newton (University of California San Diego) via Addgene (Cambridge, MA; plasmid no. 14860).

Culture of human cell lines

A549 alveolar carcinoma-derived cells were obtained from ATCC (Manassas, VA) and cultured in Ham's F-12K (Kaighn's) medium (Gibco/Thermo Fisher Scientific) plus 10% fetal bovine serum (FBS) and 1× penicillin/streptomycin cell culture antibiotic mix. A549 cells were used at passage 20–25. 16HBE14o−, an SV40-immortalized ciliated bronchial epithelial cell line (134–136), was obtained from Dr. D. Gruenert (Department of Otolaryngology, University of California at San Francisco) and cultured in minimal essential media (MEM) with Earle's salts (MEME: Gibco/Thermo Fisher Scientific) plus 10% FBS and 1× penicillin/streptomycin. Cells were used within 20 passages of receipt. Calu-3 bronchial adenocarcinoma cells were obtained from ATCC and grown in MEME plus 10% FBS and 1× penicillin/streptomycin.

For ALI cultures, cells were seeded onto collagen-coated ThinCert cell culture inserts (0.4-μm pore size, transparent PET membrane, Greiner Bio-One, Germany) in 12-well plates (1.1-cm^2 surface area). After ~3–5 days of culture and confirmation of confluence and establishment of transepithelial electrical barrier (>300 ohms·cm^2), cultures were exposed to air on the apical side by removal of apical media and washing three times with PBS. Cultures were fed from the basolateral side for at least 2 weeks before use to allow for full differentiation. For cytokine release studies, ALI cultures were stimulated on the apical side only (to simulate mucosal exposure) with PMA, TNFα, or pyocyanin dissolved in sterile PBS. Cytokines were quantified from the basolateral medium.

HEK293T cells (ATCC) were cultured in high-glucose DMEM (Gibco). Transfection of A549 and HEK293T cells for heterologous expression experiments was carried out with Lipofectamine 2000 according to the manufacturer's instructions. Sequences of human *TAS2R4*, *TAS2R5*, *TAS2R14*, *TAS2R16*, *TAS2R38* (PAV functional isoform), and *TAS2R39* were cloned into pcDNA3.1 vectors containing the first 45 amino acids of the rat type 3 somatostatin receptor at the N terminus to enhance membrane expression, as described previously (103, 137). Each T2R was co-transfected with pcDNA3.1 containing Gα_{16}-gust44, a chimeric Gα protein containing the last 44 amino acids of gustducin, as described previously (137). Cells were used 24–48 h after transfection. Transfection of 16HBE cells with the protein kinase C (PKC) FRET-reporter construct CKAR (82, 83) was performed with Lipofectamine 3000; cells were used 24 h. after transfection.

Generation of primary sinonasal ALI cultures

All experimental protocols were carried out in accordance with the University of Pennsylvania School of Medicine guidelines regarding use of residual clinical material in research. Patients undergoing sinonasal surgery were recruited from the Department of Otorhinolaryngology at the University of Pennsylvania with full IRB approval (#800614), and written informed consent was obtained for all participating patients in accordance with the United States Department of Health and Human Services code of federal regulation Title 45 CFR 46.116. Exclusion criteria included a history of systemic diseases (*e.g.* Wegener's granulomatosis, sarcoidosis, and cystic fibrosis), immunodeficiencies, or use of antibiotics, oral corticosteroids, or anti-biologics (*e.g.* Xolair) within 1 month of surgery. Human sinonasal epithelial cells were enzymatically dissociated and grown to confluence in proliferation medium (DMEM/Ham's F-12 plus BEBM; Clonetics, Cambrex, East, NJ) for 7 days as described previously (27, 138). Confluent cells were dissociated and seeded on porous polyester membranes coated with BSA, type I bovine collagen, and fibronectin in cell culture inserts in LHC basal medium (Invitrogen). Culture medium was removed from the upper compartment, and basolateral media were changed to differentiation medium (1:1 DMEM/BEBM) containing human epidermal growth factor (0.5 ng/ml), epinephrine (5 ng/ml), BPE (0.13 mg/ml), hydrocortisone (0.5 ng/ml), insulin (5 ng/ml), triiodothyronine (6.5 ng/ml), and transferrin (0.5 ng/ml), supplemented with 100 units/ml penicillin, 100 g/ml streptomycin, 0.1 nM retinoic acid, and NuSerum (BD Biosciences) as described previously (27, 138).

Live cell imaging of intracellular Ca^{2+}, reactive nitrogen species production, and PKC activation

$[Ca^{2+}]_i$ and reactive nitrogen species were imaged in primary sinonasal ALIs using the Fura-2 and DAF-FM, respectively, as described previously (23, 24, 27, 139). ALI cultures were loaded with Fura-2 AM (5 μM applied apically) for 90 min followed by washing and 20 min of incubation in the dark. Cultures were similarly loaded with 10 μM DAF-FM diacetate for 90 min in the presence of 5 μM cPTIO, followed by washing to remove unloaded DAF-FM and cPTIO and incubation for 15 min prior to imaging. Imaging was performed using an Olympus IX-83 microscope (10 × 0.4 NA PlanApo objective, Olympus Life Sciences, Tokyo, Japan) equipped with a fluorescence xenon lamp (Sutter Lambda LS, Sutter Instruments, Novato, CA), excitation and emission filter wheels (Sutter Instruments), and a 16-bit Hamamatsu Orca Flash 4.0 sCMOS camera. Images were acquired using MetaFluor (Molecular Devices, Sunnyvale, CA). Dual excitation of fura-2 was carried out with 340/11-nm and 380/11-nm bandpass excitation filters, 510 long pass dichroic mirror, and 560/80 nm emission filter (set 79002-ET, Chroma Technologies, Rockingham, VT). Excitation of DAF-FM was carried out with 470/40-nm excitation filter, 495 long pass dichroic, and 525/40-nm emission filter (Chroma 49002-ET). For fura-2 $[Ca^{2+}]_i$ measurement in submerged HEK293T cells, cells grown on coverslips were loaded with 2 μM fura-2 AM for 30 min in Hanks' balanced salt solution plus 10 mM HEPES, followed by washing and imaging with a ×30 (1.05 NA)

UPLSAPO silicone immersion objective (Olympus) using MetaFluor.

Calibration of fura-2 fluorescence from primary nasal cells to $[Ca^{2+}]_i$ was carried out as described previously (123, 124, 126) using the method of Grynkiewicz *et al.* (140) and R_{min}, R_{max}, and β values empirically determined for this specific imaging system using live cells with 0-Ca^{2+} (1 mM EGTA) and high Ca^{2+} (10 mM) solutions containing 10 μg/ml ionomycin and thapsigargin. DAF-FM measurements utilized raw fluorescence values to compare experiments performed under identical conditions with identical microscope settings.

Imaging of CKAR (82, 83) was carried out on submerged cells grown on chamber slides as described previously (80) using a dual CFP and YFP filter set (89002-ET; Chroma Technologies, Rockingham, VT) with dual 430/24- and 500/20-nm excitation filters, dual 470/24- and 535/30-nm emission filters, and multipass beam splitter. Images were acquired at 10-s intervals, and background-subtracted ratios were calculated using MetaFluor.

Measurement of CBF

Whole-field CBF was measured using the Sisson-Ammons Video Analysis system (141) as described previously (27, 81, 139) at ~28–30 °C. Cultures were imaged using at 100 frames/s using a Leica DM-IL microscope (×20/0.8 NA objective) with Hoffman modulation contrast (Leica IMC). Experiments utilized Dulbecco's PBS (1.8 mM Ca^{2+}) on the apical side and HEPES-buffered Hanks' balanced salt solution supplemented with 1× MEM vitamins and amino acids on the basolateral side.

Immunofluorescence microscopy

Immunofluorescence was carried out as described previously (27), with modifications outlined below. ALI cultures were fixed in 4% formaldehyde for 20 min at room temperature, followed by blocking and permeabilization in phosphate-buffered saline (PBS) containing 1% bovine serum albumin (BSA), 5% normal donkey serum, 0.2% saponin, and 0.3% Triton X-100 for 1 h at 4 °C. A549 or 16HBE cells were fixed in 4% formaldehyde for 20 min at room temperature, followed by blocking and permeabilization in PBS containing 1% BSA, 5% normal donkey serum, 0.2% saponin, and 0.1% Triton X-100 for 30 min at 4 °C. Primary antibody incubation (1:100 for anti-T2R antibodies and 1:250 for tubulin antibodies) were carried out at 4 °C overnight. AlexaFluor-labeled donkey anti-mouse or rabbit secondary antibody incubation (1:1000) was carried out for 2 h at 4 °C. Transwell filters were removed from the plastic mounting ring and mounted with Fluoroshield with DAPI (Abcam). For direct labeling of primary antibodies to co-localize T2R38 and T2R14, Zenon antibody labeling kits (Invitrogen/Molecular Probes/Thermo Fisher Scientific) were used according to the manufacturer's instructions. Images of ALIs were taken on an Olympus Fluoview confocal system with IX-81 microscope and ×60 (1.4 NA) objective. Images of A549 and 16HBE cells were taken in wide field with a ×60 (1.4 NA oil) objective on an Olympus IX-83 inverted microscope running Metamorph. Images were analyzed using Metamorph, Fluoview software, and/or FIJI (142)/ImageJ (W. Rasband, Research Services Branch, National Institute of Mental Health, Bethesda).

Data analysis and statistics

One-way ANOVA was performed in GraphPad Prism with appropriate post-tests as indicated; $p < 0.05$ was considered statistically significant. For comparisons of all samples within a data set, Tukey-Kramer post-test was used. For preselected pairwise comparisons, Bonferroni post-test was performed. For comparisons to a single control group, one-way ANOVA with Dunnett's post-test was used. All other data analysis was performed in Excel. For all figures, one asterisk (*) indicates $p < 0.05$ and two asterisks or pound signs (** or ##) indicate $p < 0.01$, respectively; "*n.s.*" indicates no statistical significance. All data are presented as mean ± S.E.

References

1. Stevens, W. W., Lee, R. J., Schleimer, R. P., and Cohen, N. A. (2015) Chronic rhinosinusitis pathogenesis. *J. Allergy Clin. Immunol.* **136,** 1442–1453

2. Lee, R. J., and Cohen, N. A. (2015) Role of the bitter taste receptor T2R38 in upper respiratory infection and chronic rhinosinusitis. *Curr. Opin. Allergy Clin. Immunol.* **15,** 14–20

3. Hariri, B. M., and Cohen, N. A. (2016) New insights into upper airway innate immunity. *Am. J. Rhinol. Allergy* **30,** 319–323

4. Alanis, A. J. (2005) Resistance to antibiotics: are we in the post-antibiotic era? *Arch. Med. Res.* **36,** 697–705

5. Cherry, D. K., and Woodwell, D. A. (2002) National Ambulatory Medical Care Survey: 2000 summary. *Adv. Data* 2002, **328,** 1–32

6. Ly, N., and McCaig, L. F. (2002) National Hospital Ambulatory Medical Care Survey: 2000 outpatient department summary. *Adv. Data*, 2002, **327,** 1–27

7. Ray, N. F., Baraniuk, J. N., Thamer, M., Rinehart, C. S., Gergen, P. J., Kaliner, M., Josephs, S., and Pung, Y. H. (1999) Healthcare expenditures for sinusitis in 1996: contributions of asthma, rhinitis, and other airway disorders. *J. Allergy Clin. Immunol.* **103,** 408–414

8. Bhattacharyya, N., Grebner, J., and Martinson, N. G. (2012) Recurrent acute rhinosinusitis: epidemiology and health care cost burden. *Otolaryngol. Head Neck Surg.* **146,** 307–312

9. Marcinkiewicz, J., Strus, M., and Pasich, E. (2013) Antibiotic resistance: a "dark side" of biofilmassociated chronic infections. *Pol. Arch. Med. Wewn.* **123,** 309–313

10. Kennedy, J. L., and Borish, L. (2013) Chronic rhinosinusitis and antibiotics: the good, the bad, and the ugly. *Am. J. Rhinol. Allergy* **27,** 467–472

11. Settipane, R. A., Peters, A. T., and Chandra, R. (2013) Chapter 4: Chronic rhinosinusitis. *Am. J. Rhinol. Allergy* **27,** S11–S15

12. Manes, R. P., and Batra, P. S. (2012) Bacteriology and antibiotic resistance in chronic rhinosinusitis. *Facial Plast. Surg. Clin. North Am.* **20,** 87–91

13. Godoy, J. M., Godoy, A. N., Ribalta, G., and Largo, I. (2011) Bacterial pattern in chronic sinusitis and cystic fibrosis. *Otolaryngol. Head Neck Surg.* **145,** 673–676

14. Bhattacharyya, N., and Kepnes, L. J. (2008) Assessment of trends in antimicrobial resistance in chronic rhinosinusitis. *Ann. Otol. Rhinol. Laryngol.* **117,** 448–452

15. Kingdom, T. T., and Swain, R. E., Jr. (2004) The microbiology and antimicrobial resistance patterns in chronic rhinosinusitis. *Am. J. Otolaryngol.* **25,** 323–328

16. Knowles, M. R., and Boucher, R. C. (2002) Mucus clearance as a primary innate defense mechanism for mammalian airways. *J. Clin. Invest.* **109,** 571–577

17. Majima, Y., Sakakura, Y., Matsubara, T., and Miyoshi, Y. (1986) Possible mechanisms of reduction of nasal mucociliary clearance in chronic sinusitis. *Clin. Otolaryngol. Allied Sci.* **11,** 55–60

18. Braverman, I., Wright, E. D., Wang, C. G., Eidelman, D., and Frenkiel, S. (1998) Human nasal ciliary-beat frequency in normal and chronic sinusitis subjects. *J. Otolaryngol.* **27,** 145–152

19. Chen, B., Shaari, J., Claire, S. E., Palmer, J. N., Chiu, A. G., Kennedy, D. W., and Cohen, N. A. (2006) Altered sinonasal ciliary dynamics in chronic rhinosinusitis. *Am. J. Rhinol.* **20,** 325–329

20. Atsuta, S., and Majima, Y. (1998) Nasal mucociliary clearance of chronic sinusitis in relation to rheological properties of nasal mucus. *Ann. Otol. Rhinol. Laryngol.* **107,** 47–51

21. Dejima, K., Randell, S. H., Stutts, M. J., Senior, B. A., and Boucher, R. C. (2006) Potential role of abnormal ion transport in the pathogenesis of chronic sinusitis. *Arch. Otolaryngol. Head Neck Surg.* **132,** 1352–1362

22. Lee, R. J., and Cohen, N. A. (2015) Taste receptors in innate immunity. *Cell. Mol. Life Sci.* **72,** 217–236

23. Lee, R. J., Chen, B., Redding, K. M., Margolskee, R. F., and Cohen, N. A. (2014) Mouse nasal epithelial innate immune responses to *Pseudomonas aeruginosa* quorum-sensing molecules require taste signaling components. *Innate Immun.* **20,** 606–617

24. Lee, R. J., Kofonow, J. M., Rosen, P. L., Siebert, A. P., Chen, B., Doghramji, L., Xiong, G., Adappa, N. D., Palmer, J. N., Kennedy, D. W., Kreindler, J. L., Margolskee, R. F., and Cohen, N. A. (2014) Bitter and sweet taste receptors regulate human upper respiratory innate immunity. *J. Clin. Invest.* **124,** 1393–1405

25. Lee, R. J., and Cohen, N. A. (2014) Bitter and sweet taste receptors in the respiratory epithelium in health and disease. *J. Mol. Med.* **92,** 1235–1244

26. Lee, R. J., and Cohen, N. A. (2013) The emerging role of the bitter taste receptor T2R38 in upper respiratory infection and chronic rhinosinusitis. *Am. J. Rhinol. Allergy* **27,** 283–286

27. Lee, R. J., Xiong, G., Kofonow, J. M., Chen, B., Lysenko, A., Jiang, P., Abraham, V., Doghramji, L., Adappa, N. D., Palmer, J. N., Kennedy, D. W., Beauchamp, G. K., Doulias, P.-T., Ischiropoulos, H., Kreindler, J. L., *et al.* (2012) T2R38 taste receptor polymorphisms underlie susceptibility to upper respiratory infection. *J. Clin. Invest.* **122,** 4145–4159

28. Salathe, M. (2007) Regulation of mammalian ciliary beating. *Annu. Rev. Physiol.* **69,** 401–422

29. Marcinkiewicz, J. (1997) Nitric oxide and antimicrobial activity of reactive oxygen intermediates. *Immunopharmacology* **37,** 35–41

30. Fang, F. C. (1997) Perspectives series: host/pathogen interactions. Mechanisms of nitric oxide-related antimicrobial activity. *J. Clin. Invest.* **99,** 2818–2825

31. Zhang, Y., Endam, L. M., Filali-Mouhim, A., Bossé, Y., Castano, R., and Desrosiers, M. (2011) Polymorphisms in the nitric-oxide synthase 1 gene are associated with severe chronic rhinosinusitis. *Am. J. Rhinol. Allergy* **25,** e49–e54

32. Bufe, B., Breslin, P. A., Kuhn, C., Reed, D. R., Tharp, C. D., Slack, J. P., Kim, U. K., Drayna, D., and Meyerhof, W. (2005) The molecular basis of individual differences in phenylthiocarbamide and propylthiouracil bitterness perception. *Curr. Biol.* **15,** 322–327

33. Adappa, N. D., Truesdale, C. M., Workman, A. D., Doghramji, L., Mansfield, C., Kennedy, D. W., Palmer, J. N., Cowart, B. J., and Cohen, N. A. (2016) Correlation of T2R38 taste phenotype and *in vitro* biofilm formation from nonpolypoid chronic rhinosinusitis patients. *Int. Forum Allergy Rhinol.* **6,** 783–791

34. Adappa, N. D., Zhang, Z., Palmer, J. N., Kennedy, D. W., Doghramji, L., Lysenko, A., Reed, D. R., Scott, T., Zhao, N. W., Owens, D., Lee, R. J., and

Cohen, N. A. (2014) The bitter taste receptor T2R38 is an independent risk factor for chronic rhinosinusitis requiring sinus surgery. *Int. Forum Allergy Rhinol.* **4,** 3–7

35. Adappa, N. D., Howland, T. J., Palmer, J. N., Kennedy, D. W., Doghramji, L., Lysenko, A., Reed, D. R., Lee, R. J., and Cohen, N. A. (2013) Genetics of the taste receptor T2R38 correlates with chronic rhinosinusitis necessitating surgical intervention. *Int. Forum Allergy Rhinol.* **3,** 184–187

36. Adappa, N. D., Farquhar, D., Palmer, J. N., Kennedy, D. W., Doghramji, L., Morris, S. A., Owens, D., Mansfield, C., Lysenko, A., Lee, R. J., Cowart, B. J., Reed, D. R., and Cohen, N. A. (2016) TAS2R38 genotype predicts surgical outcome in nonpolypoid chronic rhinosinusitis. *Int. Forum Allergy Rhinol.* **6,** 25–33

37. Li, F. (2013) Taste perception: from the tongue to the testis. *Mol. Hum. Reprod.* **19,** 349–360

38. Yamamoto, K., and Ishimaru, Y. (2013) Oral and extra-oral taste perception. *Semin. Cell Dev. Biol.* **24,** 240–246

39. Mfuna Endam, L., Filali-Mouhim, A., Boisvert, P., Boulet, L. P., Bossé, Y., and Desrosiers, M. (2014) Genetic variations in taste receptors are associated with chronic rhinosinusitis: a replication study. *Int. Forum Allergy Rhinol.* **4,** 200–206

40. Gallo, S., Grossi, S., Montrasio, G., Binelli, G., Cinquetti, R., Simmen, D., Castelnuovo, P., and Campomenosi, P. (2016) TAS2R38 taste receptor gene and chronic rhinosinusitis: new data from an Italian population. *BMC Med. Genet.* **17,** 54

41. Dzaman, K., Zagor, M., Sarnowska, E., Krzeski, A., and Kantor, I. (2016) The correlation of TAS2R38 gene variants with higher risk for chronic rhinosinusitis in Polish patients. *Otolaryngol. Pol.* **70,** 13–18

42. Rom, D. I., Christensen, J. M., Alvarado, R., Sacks, R., and Harvey, R. J. (2017) The impact of bitter taste receptor genetics on culturable bacteria in chronic rhinosinusitis. *Rhinology* **55,** 90–94

43. Lossow, K., Hübner, S., Roudnitzky, N., Slack, J. P., Pollastro, F., Behrens, M., and Meyerhof, W. (2016) Comprehensive analysis of mouse bitter taste receptors reveals different molecular receptive ranges for orthologous receptors in mice and humans. *J. Biol. Chem.* **291,** 15358–15377

44. Maurer, S., Wabnitz, G. H., Kahle, N. A., Stegmaier, S., Prior, B., Giese, T., Gaida, M. M., Samstag, Y., and Hänsch, G. M. (2015) Tasting *Pseudomonas aeruginosa* Biofilms: human neutrophils express the bitter receptor T2R38 as sensor for the quorum sensing molecule *N*-(3-oxododecanoyl)-L-homoserine lactone. *Front. Immunol.* **6,** 369

45. Gaida, M. M., Dapunt, U., and Hänsch, G. M. (2016) Sensing developing biofilms: the bitter receptor T2R38 on myeloid cells. *Pathog. Dis.* **74,** ftw004

46. Cushnie, T. P., and Lamb, A. J. (2011) Recent advances in understanding the antibacterial properties of flavonoids. *Int. J. Antimicrob. Agents* **38,** 99–107

47. Orhan, D. D., Özçelik, B., Özgen, S., and Ergun, F. (2010) Antibacterial, antifungal, and antiviral activities of some flavonoids. *Microbiol. Res.* **165,** 496–504

48. Martens, S., and Mithöfer, A. (2005) Flavones and flavone synthases. *Phytochemistry* **66,** 2399–2407

49. Havsteen, B. H. (2002) The biochemistry and medical significance of the flavonoids. *Pharmacol. Ther.* **96,** 67–202

50. Seleem, D., Pardi, V., and Murata, R. M. (2017) Review of flavonoids: A diverse group of natural compounds with anti-*Candida albicans* activity *in vitro*. *Arch. Oral Biol.* **76,** 76–83

51. Jiang, N., Doseff, A. I., and Grotewold, E. (2016) Flavones: from biosynthesis to health benefits. *Plants* **5,** E27

52. Wu, D., Kong, Y., Han, C., Chen, J., Hu, L., Jiang, H., and Shen, X. (2008) D-Alanine:D-alanine ligase as a new target for the flavonoids quercetin and apigenin. *Int. J. Antimicrob. Agents* **32,** 421–426

53. Sato, Y., Shibata, H., Arai, T., Yamamoto, A., Okimura, Y., Arakaki, N., and Higuti, T. (2004) Variation in synergistic activity by flavone and its related compounds on the increased susceptibility of various strains of methicillin-resistant *Staphylococcus aureus* to β-lactam antibiotics. *Int. J. Antimicrob. Agents* **24,** 226–233

54. Dao, T. T., Oh, J. W., Chi, Y. S., Kim, H. P., Sin, K. S., and Park, H. (2003) Synthesis and PGE2 inhibitory activity of vinylated and allylated chrysin analogues. *Arch. Pharm. Res.* **26,** 581–584

55. Liu, L. X., Durham, D. G., and Richards, R. M. (2001) Vancomycin resistance reversal in enterococci by flavonoids. *J. Pharm. Pharmacol.* **53,** 129–132

56. Caltagirone, S., Rossi, C., Poggi, A., Ranelletti, F. O., Natali, P. G., Brunetti, M., Aiello, F. B., and Piantelli, M. (2000) Flavonoids apigenin and quercetin inhibit melanoma growth and metastatic potential. *Int. J. Cancer* **87,** 595–600

57. Sato, M., Fujiwara, S., Tsuchiya, H., Fujii, T., Iinuma, M., Tosa, H., and Ohkawa, Y. (1996) Flavones with antibacterial activity against cariogenic bacteria. *J. Ethnopharmacol.* **54,** 171–176

58. Hariri, B. M., Payne, S. J., Chen, B., Mansfield, C., Doghramji, L. J., Adappa, N. D., Palmer, J. N., Kennedy, D. W., Niv, M. Y., and Lee, R. J. (2016) *In vitro* effects of anthocyanidins on sinonasal epithelial nitric oxide production and bacterial physiology. *Am. J. Rhinol. Allergy* **30,** 261–268

59. Suresh Babu, K., Hari Babu, T., Srinivas, P. V., Hara Kishore, K., Murthy, U. S., and Rao, J. M. (2006) Synthesis and biological evaluation of novel C (7) modified chrysin analogues as antibacterial agents. *Bioorg. Med. Chem. Lett.* **16,** 221–224

60. Ullah Mughal, E., Ayaz, M., Hussain, Z., Hasan, A., Sadiq, A., Riaz, M., Malik, A., Hussain, S., and Choudhary, M. I. (2006) Synthesis and antibacterial activity of substituted flavones, 4-thioflavones and 4-iminoflavones. *Bioorg. Med. Chem.* **14,** 4704–4711

61. Roland, W. S., van Buren, L., Gruppen, H., Driesse, M., Gouka, R. J., Smit, G., and Vincken, J. P. (2013) Bitter taste receptor activation by flavonoids and isoflavonoids: modeled structural requirements for activation of hTAS2R14 and hTAS2R39. *J. Agric. Food Chem.* **61,** 10454–10466

62. Wiener, A., Shudler, M., Levit, A., and Niv, M. Y. (2012) BitterDB: a database of bitter compounds. *Nucleic Acids Res.* **40,** D413–D419

63. Zhang, X. W., Li, W. F., Li, W. W., Ren, K. H., Fan, C. M., Chen, Y. Y., and Shen, Y. L. (2011) Protective effects of the aqueous extract of *Scutellaria baicalensis* against acrolein-induced oxidative stress in cultured human umbilical vein endothelial cells. *Pharm. Biol.* **49,** 256–261

64. Roland, W. S., Sanders, M. P., van Buren, L., Gouka, R. J., Gruppen, H., Vincken, J. P., and Ritschel, T. (2015) Snooker structure-based pharmacophore model explains differences in agonist and blocker binding to bitter receptor hTAS2R39. *PLoS ONE* **10,** e0118200

65. Roland, W. S., Gouka, R. J., Gruppen, H., Driesse, M., van Buren, L., Smit, G., and Vincken, J. P. (2014) 6-Methoxyflavanones as bitter taste receptor blockers for hTAS2R39. *PLoS ONE* **9,** e94451

66. Diaz-Meco, M. T., and Moscat, J. (2012) The atypical PKCs in inflammation: NF-κB and beyond. *Immunol. Rev.* **246,** 154–167

67. Navarro-González, J. F., and Mora-Fernández, C. (2011) Inflammatory pathways. *Contrib. Nephrol.* **170,** 113–123

68. Aksoy, E., Goldman, M., and Willems, F. (2004) Protein kinase Cε: a new target to control inflammation and immune-mediated disorders. *Int. J. Biochem. Cell Biol.* **36,** 183–188

69. Gamet-Payrastre, L., Manenti, S., Gratacap, M. P., Tulliez, J., Chap, H., and Payrastre, B. (1999) Flavonoids and the inhibition of PKC and PI 3-kinase. *Gen. Pharmacol.* **32,** 279–286

70. Ferriola, P. C., Cody, V., and Middleton, E., Jr. (1989) Protein kinase C inhibition by plant flavonoids. Kinetic mechanisms and structure-activity relationships. *Biochem. Pharmacol.* **38,** 1617–1624

71. Caramori, G., Casolari, P., Di Gregorio, C., Saetta, M., Baraldo, S., Boschetto, P., Ito, K., Fabbri, L. M., Barnes, P. J., Adcock, I. M., Cavallesco, G., Chung, K. F., and Papi, A. (2009) MUC5AC expression is increased in bronchial submucosal glands of stable COPD patients. *Histopathology* **55,** 321–331

72. Martínez-Antón, A., Debolós, C., Garrido, M., Roca-Ferrer, J., Barranco, C., Alobid, I., Xaubet, A., Picado, C., and Mullol, J. (2006) Mucin genes have different expression patterns in healthy and diseased upper airway mucosa. *Clin. Exp. Allergy* **36,** 448–457

73. Song, J. S., Kang, C. M., Yoo, M. B., Kim, S. J., Yoon, H. K., Kim, Y. K., Kim, K. H., Moon, H. S., and Park, S. H. (2007) Nitric oxide induces MUC5AC mucin in respiratory epithelial cells through PKC and ERK dependent pathways. *Respir. Res.* **8,** 28

74. Maniscalco, M., Sofia, M., and Pelaia, G. (2007) Nitric oxide in upper airways inflammatory diseases. *Inflamm. Res.* **56,** 58–69

75. Eynott, P. R., Paavolainen, N., Groneberg, D. A., Noble, A., Salmon, M., Nath, P., Leung, S. Y., and Chung, K. F. (2003) Role of nitric oxide in chronic allergen-induced airway cell proliferation and inflammation. *J. Pharmacol. Exp. Ther.* **304,** 22–29

76. Fischer, A., Folkerts, G., Geppetti, P., and Groneberg, D. A. (2002) Mediators of asthma: nitric oxide. *Pulm. Pharmacol. Ther.* **15,** 73–81

77. Nathan, C. (1997) Inducible nitric-oxide synthase: what difference does it make? *J. Clin. Invest.* **100,** 2417–2423

78. Zhang, Q., Church, J. E., Jagnandan, D., Catravas, J. D., Sessa, W. C., and Fulton, D. (2006) Functional relevance of Golgi- and plasma membrane-localized endothelial NO synthase in reconstituted endothelial cells. *Arterioscler. Thromb. Vasc. Biol.* **26,** 1015–1021

79. Sessa, W. C., García-Cardeña, G., Liu, J., Keh, A., Pollock, J. S., Bradley, J., Thiru, S., Braverman, I. M., and Desai, K. M. (1995) The Golgi association of endothelial nitric-oxide synthase is necessary for the efficient synthesis of nitric oxide. *J. Biol. Chem.* **270,** 17641–17644

80. Lee, R. J., Workman, A. D., Carey, R. M., Chen, B., Rosen, P. L., Doghramji, L., Adappa, N. D., Palmer, J. N., Kennedy, D. W., and Cohen, N. A. (2016) Fungal aflatoxins reduce respiratory mucosal ciliary function. *Sci. Rep.* **6,** 33221

81. Lee, R. J., Chen, B., Doghramji, L., Adappa, N. D., Palmer, J. N., Kennedy, D. W., and Cohen, N. A. (2013) Vasoactive intestinal peptide regulates sinonasal mucociliary clearance and synergizes with histamine in stimulating sinonasal fluid secretion. *FASEB J.* **27,** 5094–5103

82. Gallegos, L. L., and Newton, A. C. (2011) Genetically encoded fluorescent reporters to visualize protein kinase C activation in live cells. *Methods Mol. Biol.* **756,** 295–310

83. Violin, J. D., Zhang, J., Tsien, R. Y., and Newton, A. C. (2003) A genetically encoded fluorescent reporter reveals oscillatory phosphorylation by protein kinase C. *J. Cell Biol.* **161,** 899–909

84. Nanua, S., Zick, S. M., Andrade, J. E., Sajjan, U. S., Burgess, J. R., Lukacs, N. W., and Hershenson, M. B. (2006) Quercetin blocks airway epithelial cell chemokine expression. *Am. J. Respir. Cell Mol. Biol.* **35,** 602–610

85. Denning, G. M., Wollenweber, L. A., Railsback, M. A., Cox, C. D., Stoll, L. L., and Britigan, B. E. (1998) *Pseudomonas pyocyanin* increases interleukin-8 expression by human airway epithelial cells. *Infect. Immun.* **66,** 5777–5784

86. Geahlen, R. L., Koonchanok, N. M., McLaughlin, J. L., and Pratt, D. E. (1989) Inhibition of protein-tyrosine kinase activity by flavanoids and related compounds. *J. Nat. Prod.* **52,** 982–986

87. Cushman, M., Nagarathnam, D., Burg, D. L., and Geahlen, R. L. (1991) Synthesis and protein-tyrosine kinase inhibitory activities of flavonoid analogues. *J. Med. Chem.* **34,** 798–806

88. Agullo, G., Gamet-Payrastre, L., Manenti, S., Viala, C., Rémésy, C., Chap, H., and Payrastre, B. (1997) Relationship between flavonoid structure and inhibition of phosphatidylinositol 3-kinase: a comparison with tyrosine kinase and protein kinase C inhibition. *Biochem. Pharmacol.* **53,** 1649–1657

89. Suh, Y. A., Jo, S. Y., Lee, H. Y., and Lee, C. (2015) Inhibition of IL-6/STAT3 axis and targeting Axl and Tyro3 receptor tyrosine kinases by apigenin circumvent taxol resistance in ovarian cancer cells. *Int. J. Oncol.* **46,** 1405–1411

90. Kim, K. C., Choi, E. H., and Lee, C. (2014) Axl receptor tyrosine kinase is a novel target of apigenin for the inhibition of cell proliferation. *Int. J. Mol. Med.* **34,** 592–598

91. Sikder, M. A., Lee, H. J., Ryu, J., Park, S. H., Kim, J. O., Hong, J. H., Seok, J. H., and Lee, C. J. (2014) Apigenin and Wogonin regulate epidermal growth factor receptor signaling pathway involved in MUC5AC mucin gene expression and production from cultured airway epithelial cells. *Tuberc. Respir. Dis.* **76,** 120–126

92. Yeh, C. H., Yang, M. L., Lee, C. Y., Yang, C. P., Li, Y. C., Chen, C. J., and Kuan, Y. H. (2014) Wogonin attenuates endotoxin-induced prostaglandin E2 and nitric oxide production via Src-ERK1/2-NFκB pathway in BV-2 microglial cells. *Environ. Toxicol.* **29,** 1162–1170

93. Yao, J., Pan, D., Zhao, Y., Zhao, L., Sun, J., Wang, Y., You, Q. D., Xi, T., Guo, Q. L., and Lu, N. (2014) Wogonin prevents lipopolysaccharide-induced acute lung injury and inflammation in mice via peroxisome proliferator-activated receptor γ-mediated attenuation of the nuclear factor-κB pathway. *Immunology* **143,** 241–257

94. Yang, H., Hui, H., Wang, Q., Li, H., Zhao, K., Zhou, Y., Zhu, Y., Wang, X., You, Q., Guo, Q., and Lu, N. (2014) Wogonin induces cell cycle arrest and erythroid differentiation in imatinib-resistant K562 cells and primary CML cells. *Oncotarget* **5,** 8188–8201

95. Pan, M. H., Chen, W. J., Lin-Shiau, S. Y., Ho, C. T., and Lin, J. K. (2002) Tangeretin induces cell-cycle G₁ arrest through inhibiting cyclin-dependent kinases 2 and 4 activities as well as elevating Cdk inhibitors p21 and p27 in human colorectal carcinoma cells. *Carcinogenesis* **23,** 1677–1684

96. Ma, L. L., Wang, D. W., Yu, X. D., and Zhou, Y. L. (2016) Tangeretin induces cell cycle arrest and apoptosis through upregulation of PTEN expression in glioma cells. *Biomed. Pharmacother.* **81,** 491–496

97. Vaiyapuri, S., Ali, M. S., Moraes, L. A., Sage, T., Lewis, K. R., Jones, C. I., and Gibbins, J. M. (2013) Tangeretin regulates platelet function through inhibition of phosphoinositide 3-kinase and cyclic nucleotide signaling. *Arterioscler. Thromb. Vasc. Biol.* **33,** 2740–2749

98. Woo, K. J., Jeong, Y. J., Inoue, H., Park, J. W., and Kwon, T. K. (2005) Chrysin suppresses lipopolysaccharide-induced cyclooxygenase-2 expression through the inhibition of nuclear factor for IL-6 (NF-IL6) DNA-binding activity. *FEBS Lett.* **579,** 705–711

99. Kuroda, Y., Ikeda, R., Yamazaki, T., Ito, K., Uda, K., Wakabayashi, K., and Watanabe, T. (2016) Activation of human bitter taste receptors by polymethoxylated flavonoids. *Biosci. Biotechnol. Biochem.* **80,** 2014–2017

100. Huang, W., Shen, Q., Su, X., Ji, M., Liu, X., Chen, Y., Lu, S., Zhuang, H., and Zhang, J. (2016) BitterX: a tool for understanding bitter taste in humans. *Sci. Rep.* **6,** 23450

101. Shah, A. S., Ben-Shahar, Y., Moninger, T. O., Kline, J. N., and Welsh, M. J. (2009) Motile cilia of human airway epithelia are chemosensory. *Science* **325,** 1131–1134

102. Kuhn, C., and Meyerhof, W. (2013) Oligomerization of sweet and bitter taste receptors. *Methods Cell Biol.* **117,** 229–242

103. Kuhn, C., Bufe, B., Batram, C., and Meyerhof, W. (2010) Oligomerization of TAS2R bitter taste receptors. *Chem. Senses* **35,** 395–406

104. Meyerhof, W., Batram, C., Kuhn, C., Brockhoff, A., Chudoba, E., Bufe, B., Appendino, G., and Behrens, M. (2010) The molecular receptive ranges of human TAS2R bitter taste receptors. *Chem. Senses* **35,** 157–170

105. König, P., Krasteva, G., Tag, C., König, I. R., Arens, C., and Kummer, W. (2006) FRET-CLSM and double-labeling indirect immunofluorescence to detect close association of proteins in tissue sections. *Lab. Invest.* **86,** 853–864

106. Grecco, H. E., and Verveer, P. J. (2011) FRET in cell biology: still shining in the age of super-resolution? *Chemphyschem* **12,** 484–490

107. Petersen, O. H., and Tepikin, A. V. (2008) Polarized calcium signaling in exocrine gland cells. *Annu. Rev. Physiol.* **70,** 273–299

108. Greene, T. A., Alarcon, S., Thomas, A., Berdougo, E., Doranz, B. J., Breslin, P. A., and Rucker, J. B. (2011) Probenecid inhibits the human bitter taste receptor TAS2R16 and suppresses bitter perception of salicin. *PLoS ONE* **6,** e20123

109. Levit, A., Nowak, S., Peters, M., Wiener, A., Meyerhof, W., Behrens, M., and Niv, M. Y. (2014) The bitter pill: clinical drugs that activate the human bitter taste receptor TAS2R14. *FASEB J.* **28,** 1181–1197

110. Gudis, D. A., and Cohen, N. A. (2010) Cilia dysfunction. *Otolaryngol. Clin. North Am.* **43,** 461–472

111. Cohen, N. A. (2006) Sinonasal mucociliary clearance in health and disease. *Ann. Otol. Rhinol. Laryngol. Suppl.* **196,** 20–26

112. Shin, H. D., Lee, H. J., Sikder, M. A., Park, S. H., Ryu, J., Hong, J. H., Kim, J. O., Seok, J. H., and Lee, C. J. (2012) Effect of chrysin on gene expression and production of MUC5AC mucin from cultured airway epithelial cells. *Tuberc. Respir. Dis.* **73,** 204–209

113. Kim, J. O., Sikder, M. A., Lee, H. J., Rahman, M., Kim, J. H., Chang, G. T., and Lee, C. J. (2012) Phorbol ester or epidermal growth-factor-induced MUC5AC mucin gene expression and production from airway epithelial cells are inhibited by apigenin and wogonin. *Phytother. Res.* **26,** 1784–1788

114. Seo, H. S., Sikder, M. A., Lee, H. J., Ryu, J., and Lee, C. J. (2014) Apigenin inhibits tumor necrosis factor-α-induced production and gene expression of mucin through regulating nuclear factor-κB signaling pathway in airway epithelial cells. *Biomol. Ther.* **22,** 525–531

115. Sikder, M. A., Lee, H. J., Mia, M. Z., Park, S. H., Ryu, J., Kim, J. H., Min, S. Y., Hong, J. H., Seok, J. H., and Lee, C. J. (2014) Inhibition of TNF-α-induced MUC5AC mucin gene expression and production by wogonin through the inactivation of NF-κB signaling in airway epithelial cells. *Phytother. Res.* **28,** 62–68

116. Kim, D., Pauer, S. H., Yong, H. M., An, S. S., and Liggett, S. B. (2016) β2-adrenergic receptors chaperone trapped bitter taste receptor 14 to the cell surface as a heterodimer and exert unidirectional desensitization of taste receptor function. *J. Biol. Chem.* **291,** 17616–17628

117. Gahbauer, S., and Böckmann, R. A. (2016) Membrane-mediated oligomerization of G protein coupled receptors and its implications for GPCR function. *Front. Physiol.* **7,** 494

118. Ferré, S. (2015) The GPCR heterotetramer: challenging classical pharmacology. *Trends Pharmacol. Sci.* **36,** 145–152

119. Adappa, N. D., Workman, A. D., Hadjiliadis, D., Dorgan, D. J., Frame, D., Brooks, S., Doghramji, L., Palmer, J. N., Mansfield, C., Reed, D. R., and Cohen, N. A. (2016) T2R38 genotype is correlated with sinonasal quality of life in homozygous ΔF508 cystic fibrosis patients. *Int. Forum Allergy Rhinol.* **6,** 356–361

120. Zhang, S., Smith, N., Schuster, D., Azbell, C., Sorscher, E. J., Rowe, S. M., and Woodworth, B. A. (2011) Quercetin increases cystic fibrosis transmembrane conductance regulator-mediated chloride transport and ciliary beat frequency: therapeutic implications for chronic rhinosinusitis. *Am. J. Rhinol. Allergy* **25,** 307–312

121. Hartzell, C., Putzier, I., and Arreola, J. (2005) Calcium-activated chloride channels. *Annu. Rev. Physiol.* **67,** 719–758

122. Lee, R. J., and Foskett, J. K. (2012) Why mouse airway submucosal gland serous cells do not secrete fluid in response to cAMP stimulation. *J. Biol. Chem.* **287,** 38316–38326

123. Lee, R. J., and Foskett, J. K. (2010) Mechanisms of Ca^{2+}-stimulated fluid secretion by porcine bronchial submucosal gland serous acinar cells. *Am. J. Physiol. Lung Cell Mol. Physiol.* **298,** L210–L231

124. Lee, R. J., and Foskett, J. K. (2010) cAMP-activated Ca^{2+} signaling is required for CFTR-mediated serous cell fluid secretion in porcine and human airways. *J. Clin. Invest.* **120,** 3137–3148

125. Lee, R. J., Harlow, J. M., Limberis, M. P., Wilson, J. M., and Foskett, J. K. (2008) HCO3($-$) secretion by murine nasal submucosal gland serous acinar cells during Ca^{2+}-stimulated fluid secretion. *J. Gen. Physiol.* **132,** 161–183

126. Lee, R. J., Limberis, M. P., Hennessy, M. F., Wilson, J. M., and Foskett, J. K. (2007) Optical imaging of Ca^{2+}-evoked fluid secretion by murine nasal submucosal gland serous acinar cells. *J. Physiol.* **582,** 1099–1124

127. Cruickshank, S. F., Baxter, L. M., and Drummond, R. M. (2003) The Cl($-$) channel blocker niflumic acid releases Ca^{2+} from an intracellular store in rat pulmonary artery smooth muscle cells. *Br. J. Pharmacol.* **140,** 1442–1450

128. Li, L., Ma, K. T., Zhao, L., and Si, J. Q. (2008) Niflumic acid hyperpolarizes the smooth muscle cells by opening BK(Ca) channels through ryanodine-sensitive Ca^{2+} release in spiral modiolar artery. *Sheng Li Xue Bao* **60,** 743–750

129. Lee, R. J., and Cohen, N. A. (2016) Bitter taste bodyguards. *Sci. Am.* **314,** 38–43

130. Bachmanov, A. A., Bosak, N. P., Lin, C., Matsumoto, I., Ohmoto, M., Reed, D. R., and Nelson, T. M. (2014) Genetics of taste receptors. *Curr. Pharm. Des.* **20,** 2669–2683

131. Lipchock, S. V., Mennella, J. A., Spielman, A. I., and Reed, D. R. (2013) Human bitter perception correlates with bitter receptor messenger RNA expression in taste cells. *Am. J. Clin. Nutr.* **98,** 1136–1143

132. Guo, S. W., and Reed, D. R. (2001) The genetics of phenylthiocarbamide perception. *Ann. Hum. Biol.* **28,** 111–142

133. Campa, D., Vodicka, P., Pardini, B., Naccarati, A., Carrai, M., Vodickova, L., Novotny, J., Hemminki, K., Försti, A., Barale, R., and Canzian, F. (2010) A gene-wide investigation on polymorphisms in the taste receptor 2R14 (TAS2R14) and susceptibility to colorectal cancer. *BMC Med. Genet.* **11,** 88

134. Gruenert, D. C., Finkbeiner, W. E., and Widdicombe, J. H. (1995) Culture and transformation of human airway epithelial cells. *Am. J. Physiol.* **268,** L347–L360

135. Cozens, A. L., Yezzi, M. J., Kunzelmann, K., Ohrui, T., Chin, L., Eng, K., Finkbeiner, W. E., Widdicombe, J. H., and Gruenert, D. C. (1994) CFTR expression and chloride secretion in polarized immortal human bronchial epithelial cells. *Am. J. Respir. Cell Mol. Biol.* **10,** 38–47

136. Haws, C., Krouse, M. E., Xia, Y., Gruenert, D. C., and Wine, J. J. (1992) CFTR channels in immortalized human airway cells. *Am. J. Physiol.* **263,** L692–L707

137. Jiang, P., Cui, M., Zhao, B., Snyder, L. A., Benard, L. M., Osman, R., Max, M., and Margolskee, R. F. (2005) Identification of the cyclamate interaction site within the transmembrane domain of the human sweet taste receptor subunit T1R3. *J. Biol. Chem.* **280,** 34296–34305

138. Lai, Y., Chen, B., Shi, J., Palmer, J. N., Kennedy, D. W., and Cohen, N. A. (2011) Inflammation-mediated upregulation of centrosomal protein 110, a negative modulator of ciliogenesis, in patients with chronic rhinosinusitis. *J. Allergy Clin. Immunol.* **128,** 1207–1215

139. Zhao, K. Q., Cowan, A. T., Lee, R. J., Goldstein, N., Droguett, K., Chen, B., Zheng, C., Villalon, M., Palmer, J. N., Kreindler, J. L., and Cohen, N. A. (2012) Molecular modulation of airway epithelial ciliary response to sneezing. *FASEB J.* **26,** 3178–3187

140. Grynkiewicz, G., Poenie, M., and Tsien, R. Y. (1985) A new generation of Ca^{2+} indicators with greatly improved fluorescence properties. *J. Biol. Chem.* **260,** 3440–3450

141. Sisson, J. H., Stoner, J. A., Ammons, B. A., and Wyatt, T. A. (2003) All-digital image capture and whole-field analysis of ciliary beat frequency. *J. Microsc.* **211,** 103–111

142. Schindelin, J., Arganda-Carreras, I., Frise, E., Kaynig, V., Longair, M., Pietzsch, T., Preibisch, S., Rueden, C., Saalfeld, S., Schmid, B., Tinevez, J. Y., White, D. J., Hartenstein, V., Eliceiri, K., Tomancak, P., and Cardona, A. (2012) Fiji: an open-source platform for biological-image analysis. *Nat. Methods* **9,** 676–682

🔬ASBMB

J. Biol. Chem. (2017) 292(20) 8484–8497 **8497**